Elimination of Residual Flux in Transformers by the Application of an Alternating Polarity DC Voltage Source

Francisco de León, *Fellow, IEEE*, Ashkan Farazmand, Saeed Jazebi, *Member, IEEE*, Digvijay Deswal, and Raka Levi, *Senior Member, IEEE*

***Abstract*—The purpose of core demagnetization is twofold: 1) to reduce the inrush currents when transformers are energized; and 2) to make sure that the frequency-response analysis (FRA) tests are consistent to avoid false diagnoses of damage during transportation. The significance of demagnetizing is presented on field measurements of an 80 MVA unit with FRA measurements. A new demagnetizer device with an alternating polarity dc voltage source is prototyped. Experimental verification of this prototype is presented for the demagnetization of transformers. A nearly complete demagnetization was observed in the laboratory for a small single-phase isolation transformer. The method proposed in this paper is applied to three-phase transformers with different core configurations and connections. Topologically correct modeling and numerical simulations confirm the full demagnetization of all branches of three-phase (three- and five-limb) transformer cores. Inrush current measurements and FRA plots before and after demagnetization confirm the effectiveness of the process.**

***Index Terms*—Demagnetization, frequency-response analysis (FRA), inrush currents, residual flux, transformers.**

I. Introduction

INRUSH currents often emerge when a transformer is energized. Depending on transformer parameters, this transient phenomenon may last for a few cycles or seconds [1]–[4]. The magnitude of the inrush currents depends on the phase angle of the applied voltage, winding resistance, the saturation inductance (frequently called "air-core inductance") of the energized winding, and the residual flux in the core. The worst case for inrush currents is when the core has residual flux, and the switching occurs at the instant of voltage zero crossing with a polarity that increases the flux in the core. For example, in a transformer with positive residual flux, zero crossing on the transition between negative to positive polarity of voltage builds up more flux. Under this condition, the transformer core goes into super saturation [5]–[9]. This happens when the magnetizing core is completely saturated and the permeability of the magnetic material tends to unity. In such a case the iron core behaves linearly as air, and as a result, the transformer can be represented by its saturation inductance. In this condition a small incremental flux in the core tends to draw very large terminal currents. Hence, to avoid large inrush currents transformers can be demagnetized before energization.

As a diagnostic tool, frequency-response analysis (FRA) tests are performed on large power transformers in order to detect defects, such as core movement or deformation. This can occur during the transportation of the transformer or after several years of operation. Different ranges of the frequency spectrum correspond to defects associated with the core, windings, bushings, or connections [10]. The low-frequency region of the FRA is very much affected by the magnetizing status of the core [11]. The last test in the factory, performed after FRA, is the dc winding resistance test, which may leave the transformer core magnetized [12]. If the core is not properly demagnetized, the footprint of the FRA performed at the installation site is different than the one performed in the factory. This could be mistaken as a possible winding movement during transportation. Examples can be found in the CIGRE working group report [10]. Therefore, demagnetization of large power transformers in the field has become routine after performing the dc resistance tests on the windings.

A method to reduce residual flux in the core was presented in [13] using an ultra low-frequency power source. In [13], the effectiveness of the method was illustrated with numerical simulations using the Electromagnetic Transients Program (EMTP). Following a short circuit, all transformers in a feeder were demagnetized with a unit connected at the substation. A substantial reduction in the magnitude of the inrush currents was obtained.

This paper presents the demagnetization results obtained experimentally with a laboratory prototype of the power source proposed in [13]. Laboratory tests are conducted on an isolation transformer of 1 kVA, 120 V. It is demonstrated that one can successfully monitor the demagnetization process of the transformer by plotting the $\lambda - I$ curve. The results are verified by measuring the inrush currents drawn when the transformer is energized at the voltage zero crossing through a controlled switch.

Manuscript received March 17, 2014; revised October 16, 2014; accepted November 29, 2014. Date of publication December 09, 2014; date of current version July 21, 2015. Paper no. TPWRD-00299-2014.

F. de León and S. Jazebi are with the NYU Polytechnic School of Engineering, Brooklyn, NY 11201 USA (e-mail: fdeleon@nyu.edu; jazebi@ieee.org).

A. Farazmand is with TEG Energy Group, New York, NY 10003 USA (e-mail: farazmand@nyu.edu).

D. Deswal is with the Indian Institute of Technology (IIT) Kharagpur, Kharagpur, West Bengal-721302, India (e-mail: deswal.digvijay@gmail.com).

R. Levi is with DV Power, Lidingö 18125, Sweden (e-mail: Raka@dv-power.com).

Color versions of one or more of the figures in this paper are available online at http://ieeexplore.ieee.org.

Digital Object Identifier 10.1109/TPWRD.2014.2377199

In addition, it is shown by topological modeling in the EMTP that the technique works well for three-phase transformers with various core constructions and winding connections.

This paper also presents experiences accumulated with commercially available demagnetizers tested and used on transformers of up to 1100 MVA rated power and 1000 kV nominal voltage [14].

II. Available Demagnetizing Techniques and Their Performance on Large Transformers in the Field

The demagnetization of transformer cores can be performed in several ways as discussed in [13]: 1) variable voltage constant frequency (VVCF) source; 2) constant voltage variable frequency (CVVF) source; 3) decreasing the amplitude of an alternating dc current, which is a variation of the CVVF method. The latter is a modified version of the method suggested in IEEE Standard C57.152-2013 [15]. This method uses decreasing time as a measure of current.

Commercially available demagnetizers utilize a constant dc voltage source of 60 V with fast switching. The process changes the amplitude of the charging current successively in steps. Constant voltage is applied to the transformer terminal and at the moment the current reaches a preset value (for example 20 A), the supply is disconnected and a discharging circuit is connected. Once the current reaches zero, switches change the polarity of the constant voltage source applied to the terminal. This time, the source is disconnected when 60% of the previous current value is reached and consequently the discharging circuit is connected. This process is repeated until the limit of current reaches 5 mA. The method is capable of demagnetizing the largest transformers, up to 1100 MVA. The process may last from about 2 min and up to 15 min per phase depending on the size and voltage rating of the unit [16].

In this section, the experiences gained with the demagnetization of large power transformers in the field are presented. The process is illustrated with a Pauwels 80 MVA transformer, demagnetized and FRA tested on the LV side (see Figs. 1 and 2). The demagnetization process for this transformer starts by applying 60 Vdc to the winding, until 20 A current is reached. The polarity is reversed alternatively until 5 mA is reached. This is done in three stages. Each of the three events is a single-phase demagnetization process between two phases: AB, BC, and CA. Fig. 1 shows three sets of two phase currents; in the first stage, the current is applied to phase A, and returns through phase B (that is the reason why the currents are mirror images); in the second step, the current of phase B returns through phase C, and in the last step, the current of phase C returns through phase A of this delta-connected winding.

The demagnetized state of the core is demonstrated by comparing the two FRA graphs of Fig. 2. The high-frequency portion has been cut since only the low-frequency range, up to around 1 kHz, is dominated by the characteristics of the magnetic core. Fig. 2(a) shows the results after the dc winding resistance test has been performed. One can observe that there is a difference of peak amplitudes between the responses of the two outer phases (X1-X2) and (X3-X1), which should be the same for a healthy transformer. Magnetized traces may mislead the operator into believing that the core or coils are deformed or damaged.

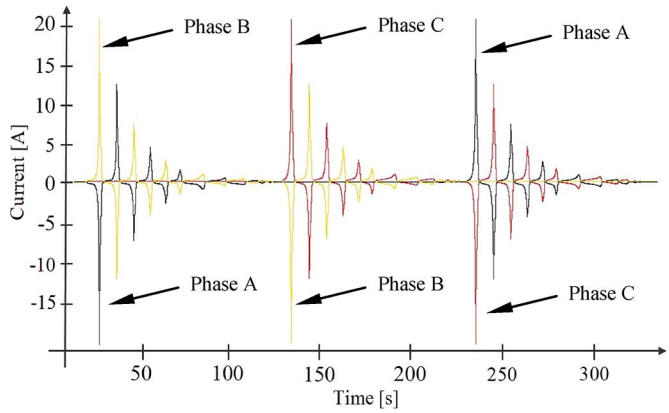

Fig. 1. Demagnetization current graph for a three-phase transformer in the field.

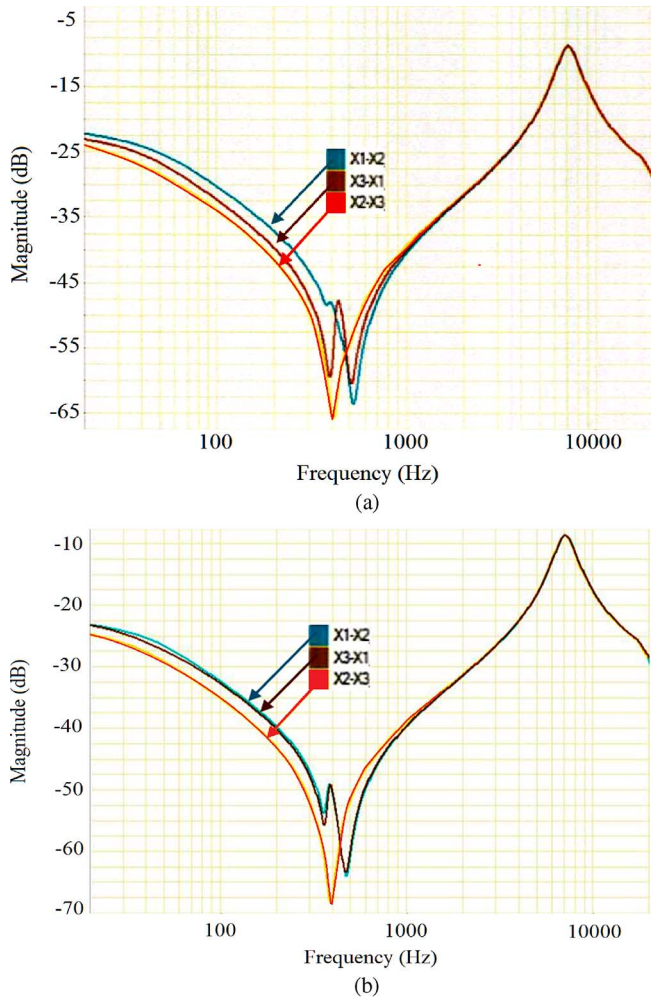

Fig. 2. FRA for a 80 MVA transformer. (a) Transformer magnetized after the dc resistance test. Note that the responses of the two external phases (X1-X2) and (X3-X1) are not identical. (b) Transformer demagnetized. Note that the responses of the two external phases (X1-X2) and (X3-X1) are now identical.

After the application of the demagnetizing technique, the normal traces of the outer phases (which should have two peaks

in this range that coincide) are seen in Fig. 2(b). One can confirm that the plots perfectly match those obtained before the dc resistance test; demonstrating the successful demagnetization of the core.

The three single-phase demagnetization processes described before has given good results in the field. The process is simple, but there is no solid proof that the demagnetization is completed. To check the demagnetization status of the core, it is necessary to perform the FRA test a second time. The setup is prolonged for a large transformer.

In conclusion, the demagnetization process with available commercial devices and techniques that are necessary to check the successfulness of the method is time consuming. The new method presented in this paper provides identical results within a few seconds.

III. Demagnetizing Device

For the physical construction of the demagnetizer in the laboratory, the more suitable technique is the CVVF; see Fig. 3. This is so because constant voltage sources are readily available. The theory behind this algorithm has been described in [13]. The demagnetizing device consists of a dc voltage source, a power-electronics switching circuit, and a controller. The functional block diagram is shown in Fig. 3(a). The basic components of each block are: 1) the switching circuit, which consists of four metal–oxide semiconductor field-effect transistors (MOSFETs) connected in the configuration shown in Fig. 4. A freewheeling diode across each MOSFET is needed to avoid instantaneous breaking of inductive currents; 2) the microcontroller and gate-drive circuits to switch the MOSFETs on/off and compute parameters such as saturation time. The microcontroller also determines saturation and demagnetization points of transformers. This is used to compute the time at which voltage reversal is executed; and 3) the current sensor, which consists of a shunt resistance to measure the current flowing in the transformer. The current waveform is used to determine the saturation of the core. A very small shunt resistance, in the range of milliohms, is used to measure the current as the resistance of the transformer winding itself is very small; 4) the signal conditioning circuit, which consists of a circuit to amplify and filter the noise out from the current signal measured across the shunt, and it also serves to condition the signal in the working range of the microcontroller; and 5) the voltage sensor, which contains a buffer circuit to prevent the loading effect on the transformer during the measurement of the induced voltage.

The practical implementation consists of the following steps, according to the procedure shown in Fig. 5:

1) Initially, all of the switches (S_1, S_2, S_3, and S_4) are off (point a). At a given instant, two opposite end switches (S_3 and S_4) are tuned on, such that negative voltage $(-V_{DC})$ is applied across the transformer until negative saturation is reached (point b). The negative saturation is detected by the shunt resistance connected in the path of switches S_3 and S_4. The sensed current is fed to the microcontroller for sampling and determining the saturation point.
2) At the negative saturation (point b), switches S_3 and S_4 are turned off and switches S_1 and S_2 are turned on. The polarity of voltage V_{DC} is reversed, so that positive voltage $(+V_{DC})$ is applied across the transformer winding. At this moment, a timer is started. The positive saturation is detected by the shunt resistance connected in the path of switches S_1 and S_2.
3) When the core reaches positive saturation (point c), switches S_1 and S_2 are turned off and switches S_3 and S_4 are again turned on. So that once again negative voltage $(-V_{DC})$ is applied across transformer windings, and time is reset to zero.
4) When the time reaches half of the recorded value in the timer, the linkage flux reaches zero (point d), and the voltage source is disconnected from the transformer.
5) The transformer is now fully demagnetized.

According to the aforementioned five steps, first the demagnetizer brings the transformer core into the negative saturation (point b). Then, the voltage changes the polarity and brings the transformer core into the positive saturation (point c). The time required to move from the negative saturation to positive saturation is T_1. Then, the voltage source changes the polarity again to

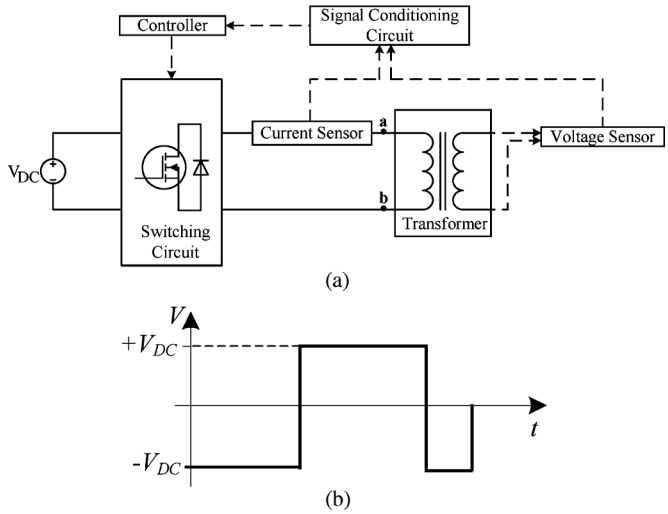

Fig. 3. (a) Demagnetization circuit for a single-phase transformerm and (b) CVVF voltage.

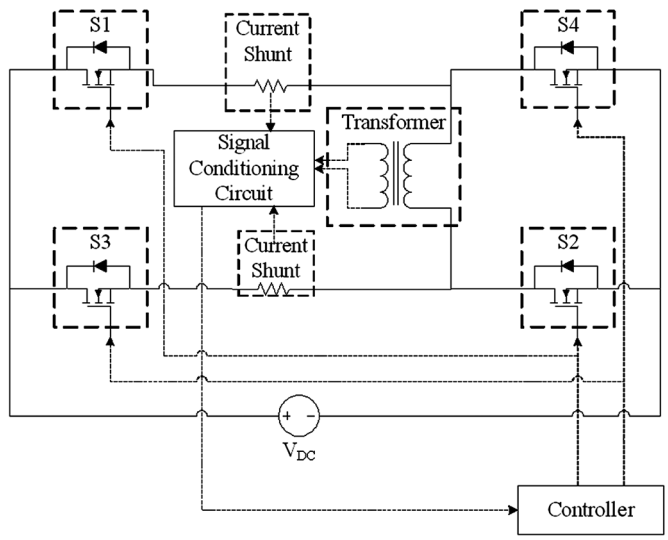

Fig. 4. Demagnetizing device circuit for single-phase transformers.

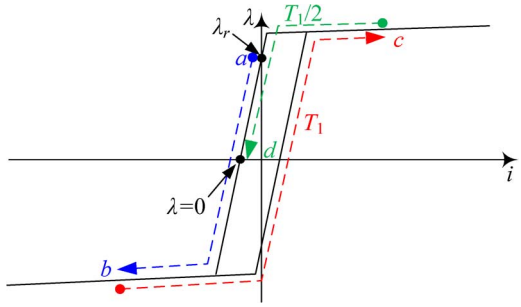

Fig. 5. Demagnetizing process from a positive residual flux.

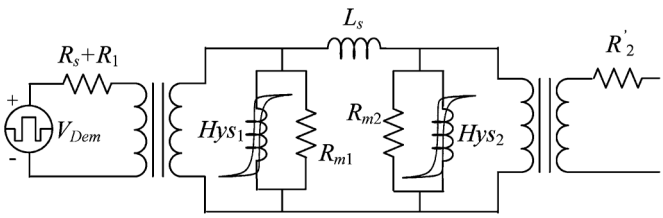

Fig. 6. Model of a single–phase transformer connected to the demagnetizer.

negative and will excite the transformer for half that time $T_1/2$. At this moment, the transformer will be demagnetized according to the $\lambda - i$ characteristic shown in Fig. 5 (point c). Therefore, there are two intervals: first $+V_{\rm DC}$ for T_1 and then $-V_{\rm DC}$ for $T_1/2$.

As discussed before, the current waveform is observed to determine the saturation point of the transformer. Consecutive samples of current are compared, and saturation is detected when the sampled current rate falls below a certain threshold. For this device, an 8 bit analog-to-digital converter (ADC) is used to sense the voltage generated due to the current passing through shunt resistances. The response is similar to that of an inductive circuit connected to a dc supply. In Section VI, a discussion on the voltage source and saturation detection is given.

IV. Demagnetizing of a Single-Phase Transformer

Demagnetization of a 1 kVA, 120 V toroidal transformer is performed using the demagnetizer via the time for saturation algorithm described before. The results of simulation using EMTP-RV [17], and experiments using the device are presented in this section.

The π model is selected to represent the single-phase transformer, which has higher accuracy compared to the conventional T model in representing the transients involving saturation of the magnetic core [1], [2], [18]. In addition, because the π model is topologically correct, its elements can be related one to one with the construction parts of the transformer core. The diagram of the circuit consists of the transformer and the demagnetizer is shown in Fig. 6. The source resistance is measured as 0.144 Ω in the laboratory.

To obtain the parameters of the transformer, the standard open circuit and impedance tests are performed [1]. The values are given in Table I. The saturation inductance of the transformer

TABLE I
Circuit Parameters for the Single–Phase Transformer

R_1 [Ω]	R'_2 [Ω]	L_s [mH]	$R_{m1} = R_{m2}$ [Ω]
0.277	0.300	0.232	2,832

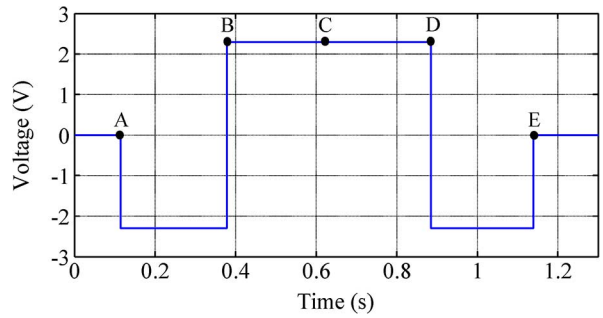

Fig. 7. Applied voltage for the single-phase transformer through the demagnetization process by the dc source.

is obtained using a nonideal low-power rectifier source in the laboratory as 314 μH [19]. This value is used to extend the hysteresis loop from the final measured point (obtained from the open circuit test) to infinity.

The applied voltage for the demagnetization process is presented in Fig. 7. The demagnetization results obtained from simulation and experiments using the demagnetization device are presented in Fig. 8. One can see good agreement between simulations and experiments. The differences are caused by the hysteresis fitter of the EMTP that are not capable of accurately reproducing the steepness of the cycle. Five points: A, B, C, D, and E are marked in Figs. 7 and 8 to describe the demagnetization process of the transformer.

Note that in the case presented here, the core is demagnetized at the beginning of the process. However, the results would be the same for any initial flux since the core goes into negative saturation first and then the time that it takes between negative and positive saturation is measured. In this example, the energization starts at point A ($t = 115$ ms) with zero flux and current (located at the center of the hysteresis cycle). At that time, a negative voltage (-2.3 V) is applied. This voltage is selected based on parameters derived from open-circuit tests and the characteristics of the voltage source (see Section VI). At point B ($t = 378$ ms), the transformer reaches negative saturation at a value of -0.57 Wb and a current of -2.4 A. Consequently, the polarity of the voltage is reversed to $+2.3$ V until the transformer goes into positive saturation. At point C, ($t = 622$ ms), the flux changes from negative to positive and the magnetizing current is 0.06 A. The voltage is still positive and linkage flux continues to build up until it gets to positive saturation ($+0.57$ Wb) at point D ($t = 0.885$) with a magnetizing current of 2.4 A.

As was explained in Section III, in order to demagnetize the transformer core, now the negative voltage must be applied for half of the time that it takes for the transformer to go from the negative saturation point to the positive saturation point. Therefore, by applying the negative voltage from $t = 885$ ms to $t = 1138$ ms, the transformer is totally demagnetized. Therefore, at point D, the polarity of the source is changed again to -2.3 V for half of the time that it took to go from point B to point D.

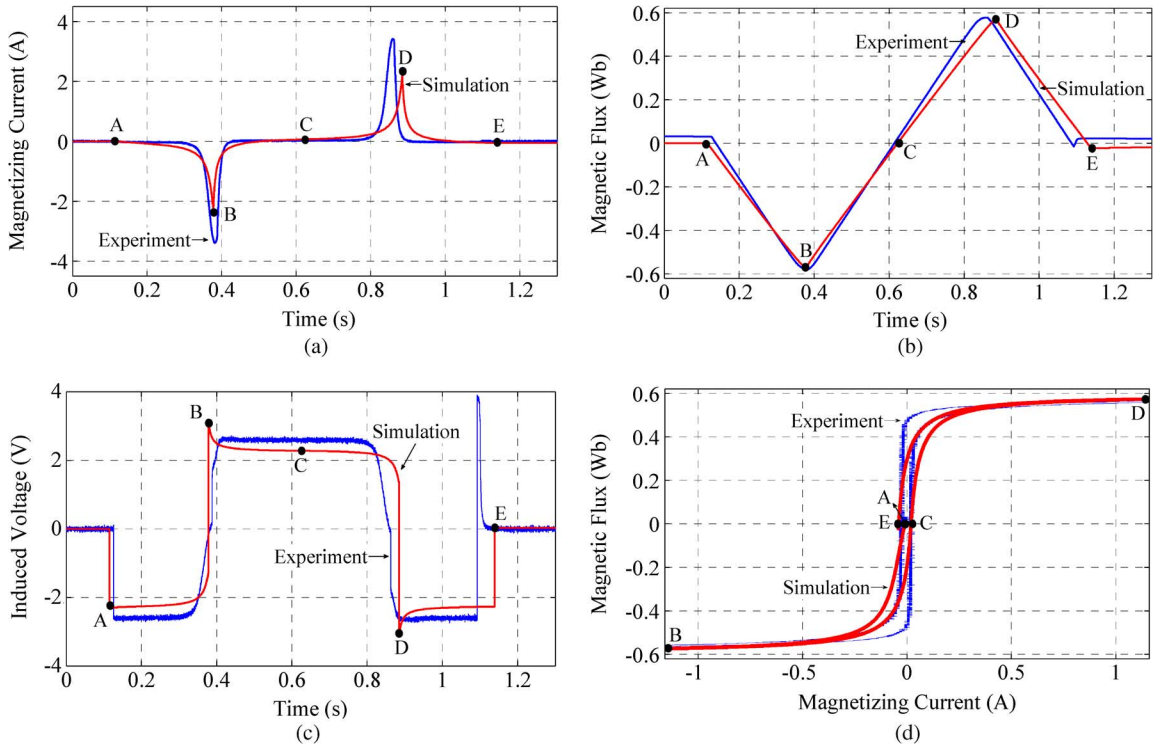

Fig. 8. Demagnetization process of a 1 kVA single-phase transformer. (a) Magnetizing current. (b) Magnetic flux. (c) Induced voltage in the open-circuited winding. (d) Hysteresis cycle.

As expected, the magnetic flux gets to zero at point E, and the transformer is demagnetized.

When positive voltage is applied across the transformer's winding, the current rises. As the flux builds up, the core starts to saturate and the value of inductance L starts to decrease. This eventually results in an abrupt rise of current at the knee point, which would be finally limited by the resistance of the transformer winding, as observed in Fig. 8(a). The slope of the flux changes from positive to negative as the polarity of the applied voltage changes [see Fig. 8(b)]. The induced voltage on the open-circuited winding is shown in Fig. 8(c), and the hysteresis loop of the transformer during the demagnetization process is presented in Fig. 8(d).

The demagnetization results were verified by performing several inrush tests using a zero-crossing switch on a demagnetized transformer. The values of inrush current were the same (254 A) for all tests. Fig. 9 presents the inrush current waveforms of the transformer obtained from experiments and simulation, which serve as additional validation of the transformer model. The peak value of the inrush current is 22 times larger than the transformer-rated current. This value could be much larger if the core is not demagnetized at the time of energization. An example of inrush current for a magnetized core is shown in Fig. 9. For this case, an initial flux of 0.45 Wb is present. As shown, the peak of inrush current is 344 A, which is 35% larger than the inrush current for the demagnetized core.

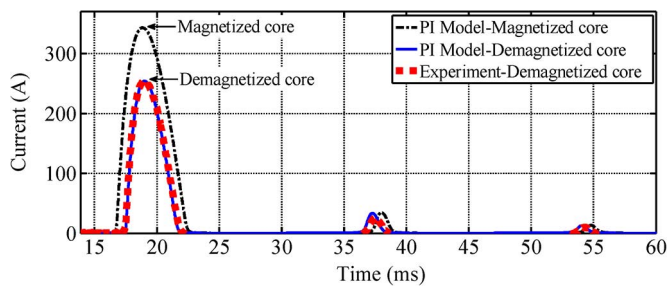

Fig. 9. Inrush current waveform of the demagnetized 1 kVA transformer.

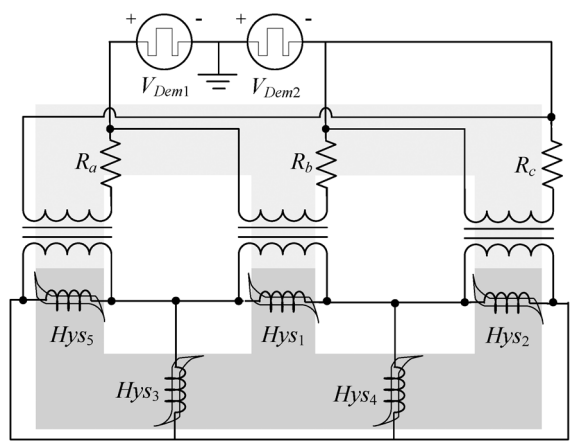

Fig. 10. Demagnetization circuit for a three-phase transformer with Δ-Y connection.

V. Demagnetizing Three-Phase Transformers

In this section, the proposed demagnetization technique is applied to three-phase transformers by simulation in the EMTP. Transformer models are obtained from the principle of duality between electric and magnetic circuits [20], [21]. In this type of model, each magnetic branch has a one-to-one relationship with

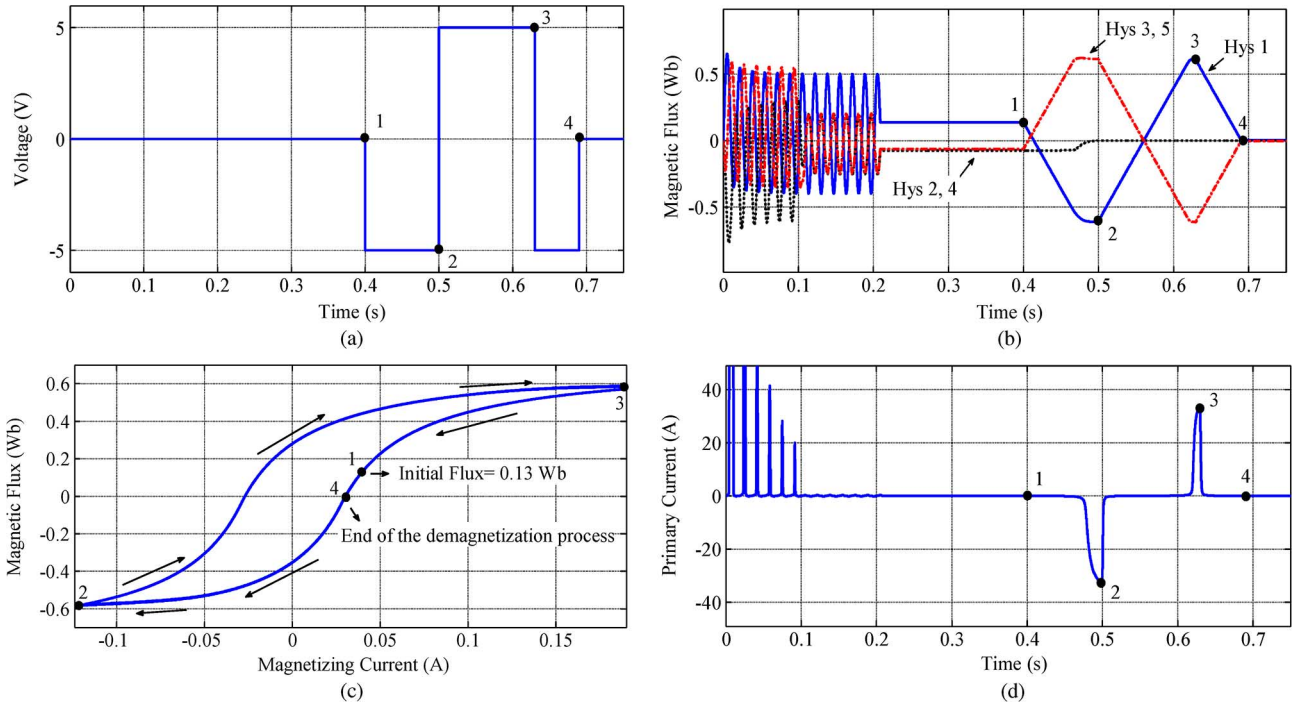

Fig. 11. Demagnetization process of the three-phase, three-leg transformer: (a) applied voltage by the dc source ($V_{\mathrm{Dem1}} = V_{\mathrm{Dem2}}$), (b) flux in all core elements, (c) hysteresis cycle (Hys 1) during the demagnetization process (after $t = 0.4$ s), and (d) terminal current.

an inductance in the electric circuit. Therefore, duality models are capable of showing the magnetizing status of each core limb and yoke.

The connection of the transformer shown in Fig. 10 is Δ-Y. Note that the secondary side is open; therefore, the secondary windings are not shown in this figure. R_a, R_b, and R_c represent the primary winding resistances. The core is modeled by five nonlinear branches using the hysteresis fitter in the EMTP-RV. By having the B–H curve of the core, the $\lambda - I$ curve is derived based on the cross-sectional area and length of each section of the transformer core [22], [23].

For three-phase transformers, only two (rather than three) alternating polarity dc sources are required. To verify the demagnetization technique with realistic remnant flux, a three-phase ac source was used to energize the transformer at $t = 0$ and disconnected at various times for each phase (before $t = 0.4$ s). During the experiments, the conditions were varied, impressing a wide range of initial conditions (residual flux) on each component of the transformer core. The applied demagnetizing voltage waveform is presented in Fig. 11(a). Four points: 1, 2, 3, and 4 are identified in Fig. 11 to present important stages of the transformer demagnetization process.

In this case, the selected dc voltage is 5 V. At $t = 0.4$ s (represented by point 1), the negative dc voltage is applied, and the transformer reaches the negative saturation 0.1 s later at point 2 ($t = 0.5$ s). The positive voltage is now applied until the transformer reaches the positive saturation at point 3 ($t = 0.63$ s). Finally, with the application of the negative dc voltage for $(0.63 - 0.5)/2 = 0.065$ s, from $t = 0.63$ to 0.695 s, and the transformer is fully demagnetized (at point 4).

From Fig. 11(b), it can be seen that all five branches are fully demagnetized after 0.69 s. Fig. 11(c) shows the hysteresis cycle of Hys 1 branch during the demagnetization process (from $t =$ 0.4 to $t = 0.7$ s). Point 1 is the initial flux as 0.13 Wb and the magnetic branch is fully demagnetized at point 4. The demagnetization process for the other four branches results in a similar hysteresis cycle. Fig. 11(d) shows the transformer primary current. The energization of the transformer at $t = 0$ with ac sources produces inrush currents (the peaks have been cut from the figure since we are interested in the demagnetization process). The transients are damped and the system reaches the steady-state condition after 0.1 s. After the transformer is disconnected from the source at $t = 0.2$ s, some flux remains on different core sections [see Fig. 11(b)]. As presented, the demagnetization process produces two peaks of current of 32.5 A when the transformer reaches its positive and negative saturation.

The demagnetizing process is also applied to a 5-limb transformer. The transformer model is derived based on the principle of duality and consists of seven nonlinear hysteresis branches; see [24]. The model is shown in Fig. 12. The applied *dc* voltage is the same as for the three-legged transformer; see Fig. 11(a). The changes in the magnetic flux during the demagnetization of the five-limb transformer with Δ-Y connection are presented in Fig. 13. This figure shows that all hysteresis branches are fully demagnetized at the end of the simulation. The hysteresis cycle and the terminal current of the transformer are not presented because of their similarity to the results obtained for the three-legged transformer shown in Fig. 11(c) and (d).

The method has been verified on Y-Y connections for three- and five-limb transformers as well. The connection strategy is shown in Fig. 14. The results are not shown for lack of space, but in all cases, all core elements are fully demagnetized.

VI. Optimal Voltage Source

In this section, the minimum voltage required to saturate the transformer is computed. The transformer is modeled as a series

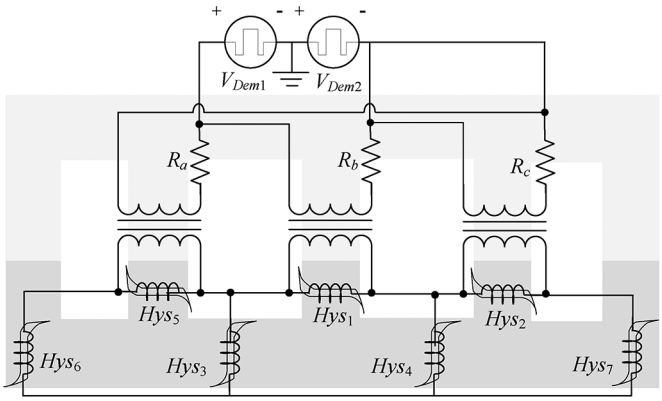

Fig. 12. Duality-derived model for a three-phase five-leg transformer used for demagnetization.

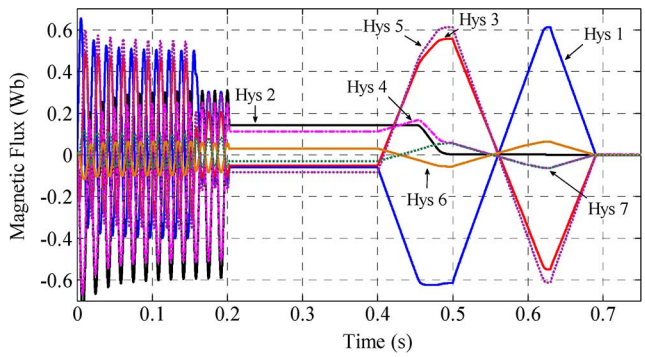

Fig. 13. Demagnetization process of a three-phase, five-limb transformer showing flux in all core elements.

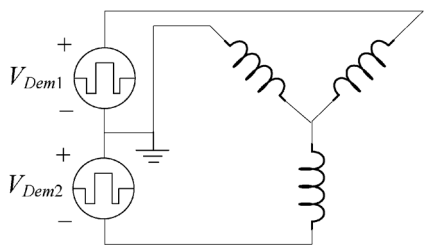

Fig. 14. Connection of demagnetizers to the transformer with Y connections.

R–L circuit. The resistance of the circuit includes the internal resistance of the source, connecting wires, and the resistance of the winding. To facilitate the analysis, the transformer magnetizing branch is modeled using a piece-wise linear inductor with two slopes. L_m (the magnetizing inductance) is for the section below the knee and L_a (the saturation inductance) is for the saturated region. L_m and L_a are derived from the standard open-circuit test [15] and saturation inductance measurements [19]. The current across the inductor includes two components: steady state (i_{ss}) and transient (i_t) as follows:

$$i(t) = i_{ss} + i_t = \frac{V_{\rm DC}}{R} + ke^{-\frac{R}{L_m}t}. \tag{1}$$

Constant k is determined from the initial conditions assuming that the transformer is disconnected from the source before demagnetization $(I_0 = 0)$, at $t = 0$

$$I_0 = \frac{V_{\rm DC}}{R} + k = 0 \rightarrow k = -\frac{V_{\rm DC}}{R}. \tag{2}$$

Hence

$$i(t) = \frac{V_{\rm DC}}{R}\left(1 - e^{-\frac{R}{L_m}t}\right) \tag{3}$$

and voltage across the inductor (V_L) is obtained as

$$V_L = L_m\frac{di}{dt} = V_{\rm DC}e^{-\frac{R}{L_m}t}. \tag{4}$$

The magnetic flux is computed by taking the integral of the voltage across the inductor, assuming that residual flux is λ_0

$$\lambda(t) = \lambda_0 + \int_{t_0}^{t} V_L(t)dt = \lambda_0 + \frac{L_m V_{\rm DC}}{R}\left(e^{-\frac{R}{L_m}t_0} - e^{-\frac{R}{L_m}t}\right). \tag{5}$$

The worst case happens when the transformer core is at the negative saturation point $\lambda_0 = -\lambda_r$, and the voltage is positive. Then, the transformer core needs to reach the saturation point at the positive side λ_s, yielding

$$-\lambda_r + \frac{L_m V_{\rm DC}}{R}\left(e^{-\frac{R}{L_m}t_0} - e^{-\frac{R}{L_m}t_s}\right) = \lambda_s. \tag{6}$$

Substituting $t_0 = 0$, the expression between the voltage of the source and the time to reach saturation is

$$V_{\rm DC} = \frac{R(\lambda_s + \lambda_r)}{L_m\left(1 - e^{-\frac{R}{L_m}t_s}\right)}. \tag{7}$$

The time to reach saturation t_s is obtained by solving (7), which yields

$$t_s = -\frac{L_m}{R}\ln\left(1 - \frac{R(\lambda_s + \lambda_r)}{V_{\rm DC}L_m}\right). \tag{8}$$

From (7) and (8), one can conclude that there is a direct relationship between the amplitude of the voltage source and the demagnetization time; the higher the voltage, the faster the demagnetization process. The minimum voltage necessary to ensure that the core will be saturated $(V_{\rm DC,min})$ is obtained by the minimization of (7), which results in

$$V_{\rm DC,min} = \frac{R(\lambda_s + \lambda_r)}{L_m}. \tag{9}$$

Also to protect the source from overcurrents, the terminal current in steady state should not exceed the nominal current of the source

$$V_{\rm DC,max} = RI_n. \tag{10}$$

Therefore, the following condition needs to be satisfied for the applied dc voltage:

$$\frac{dR(\lambda_s + \lambda_r)}{L_m} \le V_{\rm DC} \le \frac{RI_n}{d} \tag{11}$$

where $d = 1.1$ is a safety factor to ensure functionality of the device. For the single-phase transformer studied in this paper, $L_m = 1284$ mH, $R = R_1 + R_s = 277 + 144 = 421$ mΩ, $\lambda_s =$

0.57 Wb, $\lambda_r = 0.45$ Wb, and $I_n = 6$ A. Hence, the following condition needs to be satisfied:

$$0.37 \leq V_{\mathrm{DC}} \leq 2.3. \tag{12}$$

Practical experience demagnetizing large power transformers using a 60 V source shows that the time required for charging and saturating the magnetic core is in the order of 20–30 s. Up to 90 s are measured for the charging-to-saturation process of units rated at 1000 kV nominal voltage. Since the charging time depends directly on the applied dc voltage, a 60 V source is used to speed up the process. When applying this voltage, the saturation current is not limited by the resistance of the winding. The switching-off and discharge are carried out when the preprogrammed current value is reached.

VII. Conclusion

A novel-controlled power-electronics device has been designed and built to perform the demagnetization of transformer cores. Successful demagnetization of single-phase transformers has been illustrated by simulations and laboratory tests. The performance of the demagnetization has been verified experimentally with repetitive inrush current measurements.

Topological modeling and numerical simulations have shown that the demagnetizer properly removes the remanence of all magnetic branches of three- and five-limb three-phase transformers for various connections, including Δ-Y and Y-Y. The computer simulation models have been derived with the application of the principle of duality between electric and magnetic circuits and, therefore, are physically consistent. Hence, the topological models and the demagnetizer method are general and applicable for different types of transformers with various core geometry and winding connections.

References

[1] F. de León, A. Farazmand, and P. Joseph, "Comparing the T and Pi equivalent circuits for the calculation of transformer inrush currents," *IEEE Trans. Power Del.*, vol. 27, no. 4, pp. 2390–2398, Oct. 2012.

[2] S. Jazebi, F. de León, A. Farazmand, and D. Deswal, "Dual reversible transformer model for the calculation of low-frequency transients," *IEEE Trans. Power Del.*, vol. 28, no. 4, pp. 2509–2517, Oct. 2013.

[3] Y. Wang, S. G. Abdulsalam, and W. Xu, "Analytical formula to estimate the maximum inrush current," *IEEE Trans. Power Del.*, vol. 23, no. 2, pp. 1266–1268, Apr. 2008.

[4] M. Steurer and K. Frohlich, "The impact of inrush currents on the mechanical stress of high voltage power transformer coils," *IEEE Trans. Power Del.*, vol. 17, no. 1, pp. 155–160, Jan. 2002.

[5] J. H. Brunke and K. J. Frohlich, "Elimination of transformer inrush currents by controlled switching. I. Theoretical considerations," *IEEE Trans. Power Del.*, vol. 16, no. 2, pp. 276–280, Apr. 2001.

[6] J. H. Brunke and K. J. Frohlich, "Elimination of transformer inrush currents by controlled switching. II. Application and performance considerations," *IEEE Trans. Power Del.*, vol. 16, no. 2, pp. 281–285, Apr. 2001.

[7] Y. Cui, S. G. Abdulsalam, S. Chen, and W. Xu, "A sequential phase energization technique for transformer inrush current reduction—Part I: Simulation and experimental results," *IEEE Trans. Power Del.*, vol. 20, no. 2, pt. 1, pp. 943–949, Apr. 2005.

[8] W. Xu, S. G. Abdulsalam, Y. Cui, and X. Liu, "A sequential phase energization technique for transformer inrush current reduction—Part II: Theoretical analysis and design guide," *IEEE Trans. Power Del.*, vol. 20, no. 2, pt. 1, pp. 950–957, Apr. 2005.

[9] A. Farazmand, F. de León, K. Zhang, and S. Jazebi, "Analysis, modeling, and simulation of the phase-hop condition in transformers: The largest inrush currents," *IEEE Trans. Power Del.*, to be published.

[10] CIGRE Brochure 342, "Mechanical condition assessment of transformer winding using frequency response analysis (FRA)," Paris, France, Working Group A2.26 rep., 2008.

[11] N. Abeywickrama, Y. V. Serdyuk, and S. M. Gubanski, "Effect of core magnetization on Frequency Response Analysis (FRA) of power transformers," *IEEE Trans. Power Del.*, vol. 23, no. 3, pp. 1432–1438, Jul. 2008.

[12] M. F. Lachman, V. Fomichev, V. Rashkovski, and A. M. Shaikh, "Frequency response analysis of transformers and influence of magnetic viscosity," presented at the 77th Annu. Int. Doble Client Conf., Boston, MA, USA, Apr. 2010, unpublished.

[13] B. Kovan, F. de León, D. Czarkowski, Z. Zabar, and L. Birenbaum, "Mitigation of inrush currents in network transformers by reducing the residual flux with an ultra-low-frequency power source," *IEEE Trans. Power Del.*, vol. 26, no. 3, pp. 1563–1570, Jul. 2011.

[14] *"Operating Instructions DEM60C Demagnetizer,"* DV Power, Lidingo, Sweden, 2013.

[15] *IEEE Guide for Diagnostic Field Testing of Electric Power Apparatus—Part I: Oil Filled Power Transformers, Regulators, and Reactors*, IEEE Standard C57.152-2013.

[16] H. Kristensen and V. Mrdic, "Comparative analysis of three phase and single phase dynamic resistance measurement results," presented at the CIRED 22nd Int. Conf. Elect. Distrib., Stockholm, Sweden, Jun. 2013.

[17] J. Mahseredjian, S. Dennetière, L. Dubé, B. Khodabakhchian, and L. Gérin-Lajoie, "On a new approach for the simulation of transients in power systems," *Elect. Power Syst. Res.*, vol. 77, no. 11, pp. 1514–1520, Sep. 2007.

[18] S. Jazebi, A. Farazmand, B. P. Murali, and F. de León, "A comparative study on π and T equivalent models for the analysis of transformer ferroresonance," *IEEE Trans. Power Del.*, vol. 28, no. 1, pp. 526–528, Jan. 2013.

[19] F. de León, S. Jazebi, and A. Farazmand, "Accurate measurement of the air-core inductance of iron-Core transformers with a non-ideal low-power rectifier," *IEEE Trans. Power Del.*, vol. 29, no. 1, pp. 294–296, Feb. 2014.

[20] E. C. Cherry, "The duality between interlinked electric and magnetic circuits and the formation of transformer equivalent circuits," *Proc. Phys. Soc.*, vol. (B) 62, pp. 101–111, Feb. 1949.

[21] G. R. Slemon, "Equivalent circuits for transformers and machines including nonlinear effects," *Proc. Inst. Elect. Eng., IV*, vol. 100, pp. 129–143, 1953.

[22] B. A. Mork, F. Gonzalez, D. Ishchenko, D. L. Stuehm, and J. Mitra, "Hybrid transformer model for transient simulation—Part I: Development and parameters," *IEEE Trans. Power Del.*, vol. 22, no. 1, pp. 248–255, Jan. 2007.

[23] B. A. Mork, F. Gonzalez, D. Ishchenko, D. L. Stuehm, and J. Mitra, "Hybrid transformer model for transient simulation—Part II: Laboratory measurements and benchmarking," *IEEE Trans. Power Del.*, vol. 22, no. 1, pp. 256–262, Jan. 2007.

[24] C. M. Arturi, "Transient simulation and analysis of a three-phase five limb step-up transformer following and out-of-phase synchronization," *IEEE Trans. Power Del.*, vol. 6, no. 1, pp. 196–207, Jan. 1991.

Francisco de León (S'86–M'92–SM'02–F'15), photograph and biography not available at the time of publication.

Ashkan Farazmand, photograph and biography not available at the time of publication.

Saeed Jazebi (S'10–M'13), photograph and biography not available at the time of publication.

Digvijay Deswal, photograph and biography not available at the time of publication.

Raka Levi (SM'86), photograph and biography not available at the time of publication.